Chapter 2
Mathematical Morphology

Abstract MM can be defined as a theory and technique for the analysis of spatial structures, based on set theory, integral geometry and lattice algebra. It is totally different from the methods that are based on integral transform, such as FT and WT, in basic principles, algorithmic operations and approach. In contrast to the theory of linear signal processing, such as FT/WT, MM is non-linear. Moreover, it is concerned with the shape of a signal waveform in the time domain rather than the frequency domain. The emphasis of this chapter is put on the methods and theory of MM, by introducing morphological operations for signal processing. After a brief introduction of the underlying mathematical concepts, a number of morphological operators and their features and functionalities are presented.

2.1 Introduction

MM was first introduced in 1964 by two French researchers, Matheron and Serra, who worked on problems in petrography and mineralogy [125]. They introduced a set formalism to analyse binary images, which allows the image objects to be processed by simple operations such as unions, intersections, complementation and translations. In 1975, a seminal book entitled *Random Sets and Integral Geometry* was published, which is considered to have laid down the foundations of MM [99]. Having been developed for several decades, MM has become a powerful tool for signal and image processing, especially for geometrical shape analysis.

In the past 40 years, a major research topic of MM has been digital image analysis. The development in terms of methods and applications has been equally boosted and there has always been a close interconnection between them. Mature and integrated methods have been formed, such as image filtering, image segmentation and classification, image measurements, pattern recognition, and texture analysis and synthesis, etc. As for the applications of MM, it includes visual inspection and quality control, optical character recognition and document processing, materials science, geosciences, and life sciences. An overview of the development of MM can

be found in two milestone monographs by J. Serra in 1982 [125] and P. Soille in 2003 [131], respectively.

Considering its mathematical background, MM is defined on a complete lattice. Before giving the definition of a complete lattice, we need to understand the concept of a partly ordered set, which is also called a poset. A partly ordered set is a set in which a binary relation '$\leq$' is defined for certain pairs of elements. The binary relation '$\leq$' over a set $\mathscr{P}$ satisfies the following conditions for all elements $x, y, z \in \mathscr{P}$:

1. *Reflexive:* $\forall\, x, x \leq x$.
2. *Antisymmetry:* If $x \leq y$ and $y \leq x$, then $x = y$.
3. *Transitivity:* If $x \leq y$ and $y \leq z$, then $x \leq z$.

Given two partly ordered sets A and B and arbitrary elements a and x, the following definitions can be developed:

1. *Translation:* The translation of A by x, denoted by $(A)_x$, is defined as $(A)_x = \{a + x | a \in A\}$.
2. *Reflection:* The reflection of A, denoted by $\check{A}$, is defined as $\check{A} = \{-a | a \in A\}$. Reflection is also called transposition.
3. *Complement:* The complement of A, denoted by A^{c}, is defined as $A^{\mathrm{c}} = \{x | x \notin A\}$.
4. *Difference:* The difference between two sets A and B, denoted by $A - B$, is defined as $A - B = \{x | x \in A, x \notin B\} = A \bigcap B^{\mathrm{c}}$. Based on this operation, the complement of set A can also be defined as $A^{\mathrm{c}} = \{x | x \in I - A\}$, where I is the universal set.

The partially ordered set formalises the intuitive concept of an ordering relation, which plays a key role in MM [131]. Aside from partial ordering, there also exists a total ordering relation. A totally ordered set has a strengthened relation of '$<$': for any two elements x and y, exactly one of $x < y$, $x = y$, $x > y$ is true. The property of transitivity on a totally ordered set becomes $x < y$ and $y < z$ implies $x < z$.

A poset, $(\mathscr{P}, \leq)$, is a lattice if any two elements of it, x and y, have a greatest lower bound (i.e. infimum), $x \wedge y$, and a least upper bound (i.e. supremum), $x \vee y$. A lattice, $\mathscr{J}$, is a complete lattice if each of its subsets has an infimum and a supremum in $\mathscr{J}$. A complete lattice satisfies the following properties: for subsets X, Y and Z,

1. *Commutativity:* $X \vee Y = Y \vee X, X \wedge Y = Y \wedge X$.
2. *Associativity:* $(X \vee Y) \vee Z = X \vee (Y \vee Z), (X \wedge Y) \wedge Z = X \wedge (Y \wedge Z)$.

2.2 Basic Morphological Operators

2.2.1 Definitions for Binary Operations

2.2.1.1 Minkowski Addition and Subtraction

The main function of morphological operators is to extract relevant structures of a set. The extraction is usually done by the interaction between the set and another set, which is called structuring element (SE). The shape of the SE is pre-defined according to some a priori knowledge about the shape of the signal. There are two basic morphological operators, dilation and erosion, which form a pair of dual transforms. They are derived from Minkowski set theory. Therefore, we start this section from the introduction to Minkowski addition and subtraction.

Minkowski addition is a binary operation of two sets A and B in Euclidean space, named after Hermann Minkowski. It is denoted by $\overset{\mathrm{M}}{\oplus}$ and is defined as the result of adding every element of A to every element of B:

$$A \overset{\mathrm{M}}{\oplus} B = \{a+b | a \in A, b \in B\} = \bigcup_{b \in B} (A)_b. \tag{2.1}$$

It is assumed that $A \overset{\mathrm{M}}{\oplus} \{0\} = A$ and $A \overset{\mathrm{M}}{\oplus} \emptyset = \emptyset$. The dual operation is called Minkowski subtraction, denoted by $\overset{\mathrm{M}}{\ominus}$, and defined as:

$$A \overset{\mathrm{M}}{\ominus} B = \bigcap_{b \in B} (A)_b. \tag{2.2}$$

The following relation will be true for Minkowski subtraction:

$$A \overset{\mathrm{M}}{\ominus} B = \{x | (\check{B})_x \subseteq A\} = (A^{\mathrm{c}} \overset{\mathrm{M}}{\oplus} B)^{\mathrm{c}}. \tag{2.3}$$

Proof:

$$\begin{aligned}
\because \quad & z \in \left(\bigcap_{b \in B} (A)_b \right) \\
& \Rightarrow z \in (A)_b \\
& \Rightarrow z \in \{a+b | a \in A, b \in B\} \\
& \Rightarrow z \in \{x | x-b \in A, b \in B\} \\
\text{and} \ \because \quad & \{x | (\check{B})_x \subseteq A\} = \{x | x-b \in A, b \in B\} \\
\therefore \quad & A \overset{\mathrm{M}}{\ominus} B = \{x | (\check{B})_x \subseteq A\}.
\end{aligned}$$

$$\begin{aligned}\because A^{\mathrm{c}} \overset{\mathrm{M}}{\oplus} B &= \bigcup_{b\in B}(I-A)_b = I - \bigcap_{b\in B}(A)_b \\ &= \left(\bigcap_{b\in B}(A)_b\right)^{\mathrm{c}} = \left(A \overset{\mathrm{M}}{\ominus} B\right)^{\mathrm{c}} \\ \therefore\ A \overset{\mathrm{M}}{\ominus} B &= (A^{\mathrm{c}} \overset{\mathrm{M}}{\oplus} B)^{\mathrm{c}}.\end{aligned}$$

Next, we will prove that Minkowski addition satisfies the properties of commutativity and associativity. Similar methods can be used to prove that Minkowski subtraction also satisfies these properties.

1. *Commutativity:* $A \overset{\mathrm{M}}{\oplus} B = B \overset{\mathrm{M}}{\oplus} A$.
   Proof:
$$\begin{aligned}A \overset{\mathrm{M}}{\oplus} B &= \{x|x = a+b, a\in A, b\in B\} \\ &= \{x|x = b+a, b\in B, a\in A\} = B \overset{\mathrm{M}}{\oplus} A.\end{aligned}$$

2. *Associativity:* $(A \overset{\mathrm{M}}{\oplus} B) \overset{\mathrm{M}}{\oplus} C = A \overset{\mathrm{M}}{\oplus} (B \overset{\mathrm{M}}{\oplus} C)$.
   Proof:
$$\begin{aligned}A \overset{\mathrm{M}}{\oplus} (B \overset{\mathrm{M}}{\oplus} C) &= \{a+(b+c)|a\in A, b+c\in B \overset{\mathrm{M}}{\oplus} C\} \\ &= \{a+b+c|a\in A, b\in B, c\in C\} \\ &= \{(a+b)+c|a+b\in A \overset{\mathrm{M}}{\oplus} B, c\in C\} \\ &= (A \overset{\mathrm{M}}{\oplus} B) \overset{\mathrm{M}}{\oplus} C.\end{aligned}$$

2.2.1.2 Binary Dilation and Erosion

The definition of dilation is similar to Minkowski addition. Replacing the operator $\overset{\mathrm{M}}{\oplus}$ by $\oplus$ in (2.1) and use a reflected SE, $\check{B}$, we have

$$A \oplus B = \bigcup_{b\in\check{B}}(A)_b = \bigcup_{b\in B}(A)_{-b} = \bigcup_{b\in B}\{x|x = a-b, a\in A\}. \tag{2.4}$$

Erosion derives from Minkowski subtraction, but this time b comes from the reflection set of B. The definition of erosion is

$$A \ominus B = \bigcap_{b\in\check{B}}(A)_b = \bigcap_{b\in B}(A)_{-b} = \bigcap_{b\in B}\{x|x = a-b, a\in A\}. \tag{2.5}$$

Since a binary image is a digital image that has only two possible values for each pixel, it is very convenient to describe a binary image using the notion of a set. A binary image is often considered as a set I, while an object in it is considered as a subset $X \subseteq I$. Letting sets A and B represent two binary images in the above definitions, we have the operations of dilation and erosion for binary image processing.

The two images A and B function differently in image processing. Generally speaking, A is the image being processed, while B serves as an SE that slides as a

probe across image A and interacts with each pixel of A. Obviously, the size of B should be much smaller than that of A. To have a clear view of this process, we give an example in Fig. 2.1 to show how dilation and erosion function between a binary image and an SE. Here, the origin of B is set at $(0,0)$.

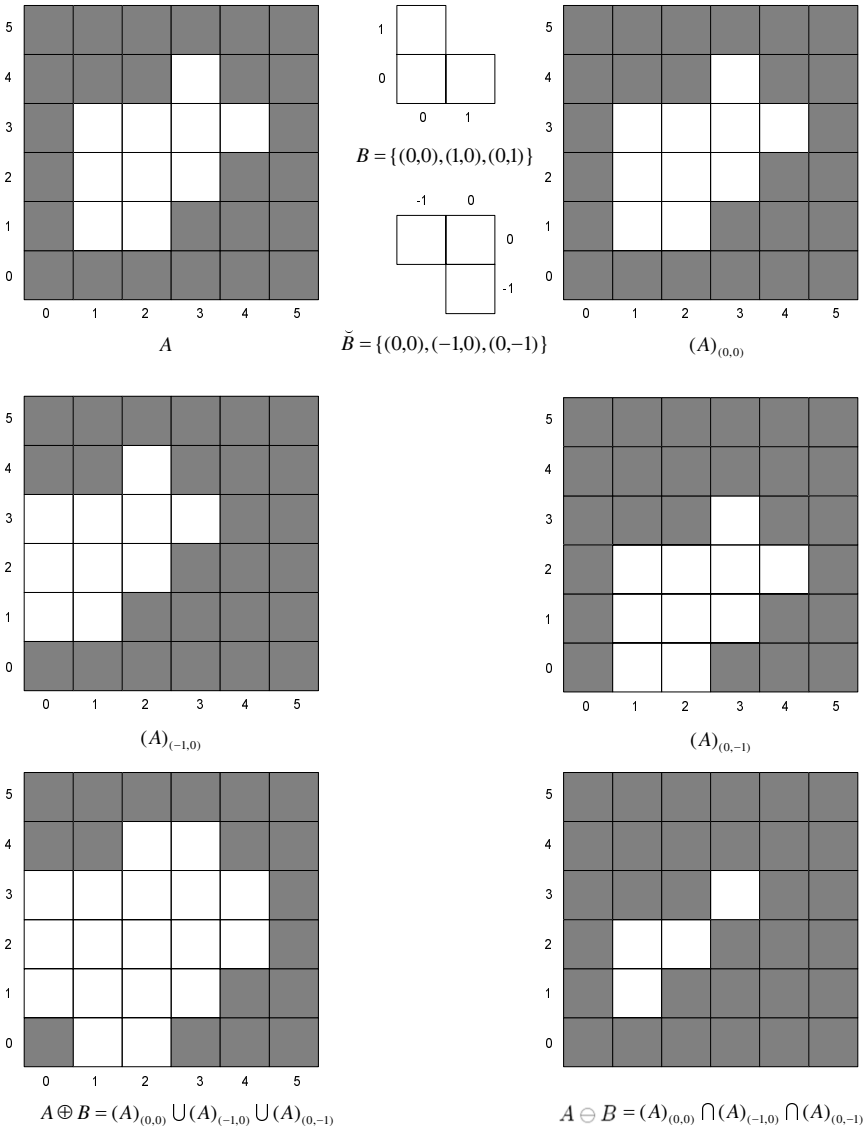

Fig. 2.1 Binary dilation and erosion of a binary image

Figure 2.1 illustrates an important property of dilation and erosion – duality, which means that applying dilation to A is equivalent to applying erosion to its complement A^c. This property can be expressed as:

$$A \oplus B = (A^c \ominus B)^c, \tag{2.6}$$

$$A \ominus B = (A^c \oplus B)^c. \tag{2.7}$$

Proof:

$$\begin{aligned} A^c \oplus B &= \bigcup_{b \in \check{B}} (I - A)_b = \bigcup_{b \in B} (I - A)_{-b} \\ &= I - \bigcap_{b \in B} (A)_{-b} \\ &= I - A \ominus B = (A \ominus B)^c \\ \Rightarrow\ A \ominus B &= (A^c \oplus B)^c. \end{aligned}$$

The property of duality illustrates that the processing of dilation and erosion is not reversible and there is no inverse transform for the operators. As we can see from the following sections, applying dilation and erosion alternately actually produces a pair of new operations.

2.2.2 Set Representations of Functions

In order to extend morphological operators to functions, the functions are represented by their umbra [132], which is defined as:

$$U(f) = \{(x, a) | a \leq f(x)\}. \tag{2.8}$$

Hence, a d-dimensional function $f(x)$ is represented by a $(d+1)$-dimensional set. Obviously, the umbra is the set of points below the surface represented by $f(x)$. After getting the umbra, binary morphological operators can be applied to the signal. In general, the umbra set extends to $a = -\infty$, and the function f can be reconstructed from its umbra since:

$$f(x) = \max\{a | (x, a) \in U(f)\},\ \forall x. \tag{2.9}$$

Figure 2.2 shows, as an example, the umbra of a sinusoidal function, where the umbra of $f(x)$ is the shaded region. We can easily show that $f \leq g \Leftrightarrow U(f) \subseteq U(g)$.

Some definitions for grey-scale operations based on sets are defined as follows [140]:

1. *Grey-scale union:* The union of two functions f and g, denoted by $f \vee g$, is defined as:

$$(f \vee g)(x) = f(x) \vee g(x). \tag{2.10}$$

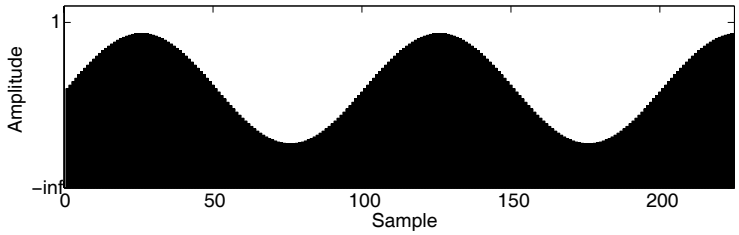

Fig. 2.2 Umbrae $U(f)$ of a sinusoidal function f

There is a one-to-one correspondence between the union of functions and the set union:

$$U(f \vee g) = U(f) \cup U(g). \tag{2.11}$$

2. *Grey-scale intersection:* The intersection of two functions f and g, denoted by $f \wedge g$, is defined as:

$$(f \wedge g)(x) = f(x) \wedge g(x). \tag{2.12}$$

A similar one-to-one correspondence exists for the function and the set intersection:

$$U(f \wedge g) = U(f) \cap U(g). \tag{2.13}$$

3. *Grey-scale transpose:* The transpose $\check{f}$ of a function f is defined as:

$$\check{f}(x) = f(-x). \tag{2.14}$$

4. *Grey-scale complement:* The complement f^{c} of a function f is defined as:

$$f^{\mathrm{c}}(x) = -f(x). \tag{2.15}$$

Notice that $f \vee f^{\mathrm{c}} = |f|$ and $f \wedge f^{\mathrm{c}} = -|f|$, whereas for sets, we have $A \cup A^{\mathrm{c}} = I$ and $A \cap A^{\mathrm{c}} = \emptyset$. Figure 2.3 shows the above properties.

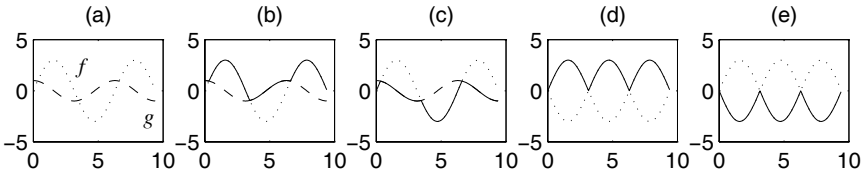

Fig. 2.3 The grey-scale operations. **a** Two functions f (*dotted line*) and g (*dashed line*). **b** $f \vee g$ (*solid line*). **c** $f \wedge g$ (*solid line*). **d** $f \vee f^{\mathrm{c}}$ (*solid line*). **e** $f \wedge f^{\mathrm{c}}$ (*solid line*)

For an eight-bit grey-scale digital image, each pixel of which can have $2^8 = 256$ possible values to carry the full and only information about its intensity, the image can be represented as a set whose components are in $\mathbb{Z}^3$. In this case, two components of each element of the set refer to the coordinates of a pixel, and the third corresponds to its discrete intensity value. For a signal, the set is defined in $\mathbb{Z}^2$ with each element corresponding to a sample of the digitised signal. Similarly, the first component of each element represents the coordinate and the second represents its value. Sets in a higher dimensional space can contain other attributes, such as the colour information of an image.

2.2.3 Grey-Scale Dilation and Erosion

In order to use MM in signal processing where most signals are not binary, morphological operators should be extended to a grey-scale level. Instead of performing dilation and erosion by union and intersection as in the binary case, they are performed by algebraic addition and subtraction in the grey-scale case. Let f denote a signal and g denote an SE, and the length of g be considerably shorter than that of f [122]. Dilation and erosion are defined as follows:

$$f \oplus g(x) = \max_s \{f(x+s) + g(s) | (x+s) \in \mathscr{D}_f, s \in \mathscr{D}_g\}, \tag{2.16}$$

$$f \ominus g(x) = \min_s \{f(x+s) - g(s) | (x+s) \in \mathscr{D}_f, s \in \mathscr{D}_g\}, \tag{2.17}$$

where $\mathscr{D}_f$, $\mathscr{D}_g$ are the definition domains of f and g, respectively. For example, suppose the SE, g, has a length of five samples with its origin in the middle. In this case, the domain of g is given by $\mathscr{D}_g = \{-2,-1,0,1,2\}$. The dilation and erosion of f by g are therefore calculated from

$$\begin{aligned} f \oplus g(x) = \max\{&f(x-2)+g(-2), f(x-1)+g(-1), f(x)+g(0), \\ &f(x+1)+g(1), f(x+2)+g(2)\}, \end{aligned}$$

and

$$\begin{aligned} f \ominus g(x) = \min\{&f(x-2)-g(-2), f(x-1)-g(-1), f(x)-g(0), \\ &f(x+1)-g(1), f(x+2)-g(2)\}, \end{aligned}$$

respectively. Intuitively, dilation can be imagined as swelling or expanding, while erosion can be thought of as a shrinking procedure. The pseudo code of dilation is given in Table 2.1. Likewise, the pseudo code of erosion can be given in a similar way by substituting 'maximum' with 'minimum', as shown in Table 2.2.

As explained previously, the SE is a small set used to probe the signal under study. A simple case is that the SE has the form of $g(s) \equiv 0$, $s \in \mathscr{D}_g$, which is referred to as a 'flat SE'. Hence, definitions of dilation and erosion degrade to:

Table 2.1 The pseudo code of dilation

Determine the SE, including its definition domain and the value of each element. Suppose $m \le s \le n$;
for (each sample of the signal $f(x)$)
  for ($m \le s \le n$)
    Calculate $\omega(s-m+1) = f(x+s)+g(s)$;
  end
  Return the maximum element of ω and $f \oplus g(x) = \max\{\omega\}$;
end

Table 2.2 The pseudo code of erosion

Determine the SE, including its definition domain and the value of each element. Suppose $m \le s \le n$;
for (each sample of the signal $f(x)$)
  for ($m \le s \le n$)
    Calculate $\varpi(s-m+1) = f(x+s)-g(s)$;
  end
  Return the minimum element of ϖ and $f \ominus g(x) = \min\{\varpi\}$;
end

$$f \oplus g(x) = \max_s\{f(x+s)|(x+s) \in \mathscr{D}_f, s \in \mathscr{D}_g\}, \tag{2.18}$$

$$f \ominus g(x) = \min_s\{f(x+s)|(x+s) \in \mathscr{D}_f, s \in \mathscr{D}_g\}. \tag{2.19}$$

The function of g is to indicate which samples are involved when processing the current sample. For a binary signal, the SE, g, must be flat. The dilation and erosion of a one-dimensional signal are illustrated in Figs. 2.4a and b, respectively. Both operations use a flat SE of length 3: $g(-1) = g(0) = g(1) = 0$.

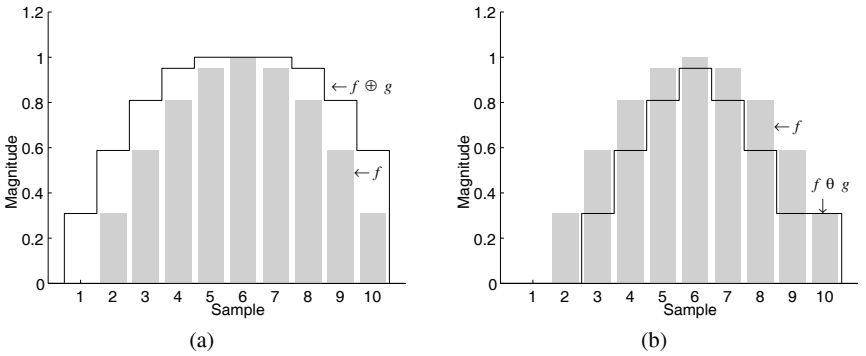

Fig. 2.4 Grey-scale dilation and erosion of a one-dimensional signal. **a** Dilation. **b** Erosion

Figure 2.4 demonstrates another property of dilation and erosion, i.e. that they are increasing transforms. The property can be expressed as follows. For two signals,

f_1 and f_2, and an arbitrary SE, g, we have:

$$f_1 \leq f_2 \Rightarrow \begin{cases} f_1 \oplus g \leq f_2 \oplus g \\ f_1 \ominus g \leq f_2 \ominus g \end{cases}. \tag{2.20}$$

The ordering relation between dilation and erosion can be expressed as the erosion of a signal by an SE being less than or equal to its dilation by the same SE: $f \ominus g \leq f \oplus g$. If the SE contains its origin, which means processing a sample of the signal within a window that contains the sample, the following ordering exists:

$$f \ominus g \leq f \leq f \oplus g. \tag{2.21}$$

2.3 Morphological Filters

2.3.1 Definitions of Morphological Filters

Morphological filters are non-linear signal transforms that locally modify the geometrical features of signals or image objects. The idempotence and increasing properties are necessary and sufficient conditions for a transform, ψ, to be a morphological filter:

ψ is a morphological filter $\Leftrightarrow$ ψ is increasing and idempotent.

The property of idempotence implies that applying a morphological filter twice to a signal is equivalent to applying it only once:

ψ is idempotent $\Leftrightarrow \psi\psi = \psi$.

The increasing property ensures that the ordering relation on signals is preserved after being filtered if the same SE is employed.

2.3.2 Opening and Closing

Opening is an operator that performs dilation on a signal eroded by the same SE. The definition is given as follows:

$$f \circ g = (f \ominus g) \oplus g, \tag{2.22}$$

where f is the signal, g is the SE, and $\circ$ denotes the opening operator. Opening can recover most structures lost by erosion, except for those completely erased by erosion. Closing, on the other hand, can be defined by its duality as:

$$f \bullet g = (f \oplus g) \ominus g. \tag{2.23}$$

Usually, opening and closing are also denoted by operators γ and ϕ, respectively. The pseudo code of opening is given in Table 2.3, and the pseudo code of closing

can be given likewise, as shown in Table 2.4. The results of performing opening and closing on the signal used in the previous section by the same SE are illustrated in Fig. 2.5.

Table 2.3 The pseudo code of opening

Determine the SE, including its definition domain and the value of each element. Suppose $m \le s \le n$;
for (each sample of the signal $f(x)$)
  for ($m \le s \le n$)
    Calculate $\varpi(s-m+1) = f(x+s) - g(s)$;
  end
  Return the minimum element of ϖ and $\varepsilon(x) = \min\{\varpi\}$;
end
for (each sample of the signal $\varepsilon(x)$)
  for ($m \le s \le n$)
    Calculate $\omega(s-m+1) = \varepsilon(x+s) + g(s)$;
  end
  Return the maximum element of ω and $\gamma(x) = \max\{\omega\}$;
end

Table 2.4 The pseudo code of closing

Determine the SE, including its definition domain and the value of each element. Suppose $m \le s \le n$;
for (each sample of the signal $f(x)$)
  for ($m \le s \le n$)
    Calculate $\omega(s-m+1) = f(x+s) + g(s)$;
  end
  Return the maximum element of ω and $\delta(x) = \max\{\omega\}$;
end
for (each sample of the signal $\delta(x)$)
  for ($m \le s \le n$)
    Calculate $\varpi(s-m+1) = \delta(x+s) - g(s)$;
  end
  Return the minimum element of ϖ and $\phi(x) = \min\{\varpi\}$;
end

Morphological opening and closing are both increasing transforms:

$$f_1 \le f_2 \Rightarrow \begin{cases} \gamma(f_1) \le \gamma(f_2) \\ \phi(f_1) \le \phi(f_2) \end{cases}. \tag{2.24}$$

Moreover, successive applications of openings or closings do not further modify the signal, which means that they are both idempotent transforms:

$$\begin{aligned} \gamma\gamma &= \gamma \\ \phi\phi &= \phi \end{aligned}. \tag{2.25}$$

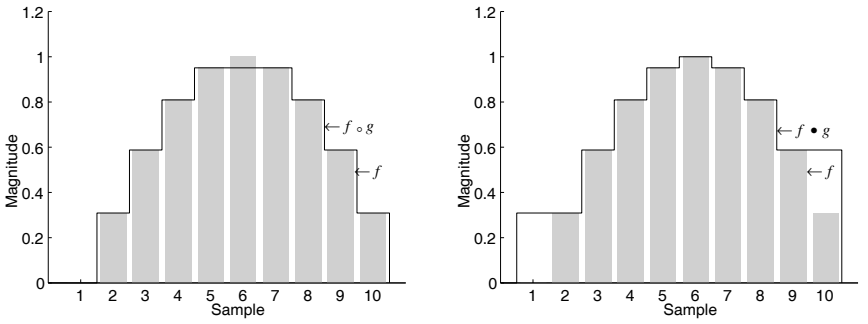

Fig. 2.5 Grey-scale opening and closing of a one-dimensional signal. **a** Opening. **b** Closing

Apparently, opening and closing fulfill the conditions of morphological filters.

Opening and closing are also a pair of dual transforms:

$$A \circ B = (A^{\mathrm{c}} \bullet B)^{\mathrm{c}}, \tag{2.26}$$

$$A \bullet B = (A^{\mathrm{c}} \circ B)^{\mathrm{c}}. \tag{2.27}$$

Proof:

$$\begin{aligned} (A \circ B)^{\mathrm{c}} &= (A \ominus B \oplus B)^{\mathrm{c}} = (A \ominus B)^{\mathrm{c}} \ominus B \\ &= A^{\mathrm{c}} \oplus B \ominus B = A^{\mathrm{c}} \bullet B \\ \Rightarrow \quad A \circ B &= (A^{\mathrm{c}} \bullet B)^{\mathrm{c}}. \end{aligned}$$

A useful operator called top-hap transform can be derived from opening, which is defined as:

$$T_{\mathrm{TH}}(f) = f - f \circ g, \tag{2.28}$$

where $T_{\mathrm{TH}}(f)$ denotes the top-hap transform of signal f. This operator is useful for enhancing the detail in the presence of shading [26].

2.3.3 Alternating Sequential Filters

Opening and closing are the basic morphological filters and new filters can be designed from their sequential combinations, such as an opening followed by a closing or vice versa. In fact, all the following combinations are filters: $\gamma\phi$, $\phi\gamma$, $\gamma\phi\gamma$ and $\phi\gamma\phi$. Moreover, for these new filters, the ordering relations of

$$\gamma \leq \gamma\phi\gamma \leq \begin{matrix} \gamma\phi \\ \phi\gamma \end{matrix} \leq \phi\gamma\phi \leq \phi \tag{2.29}$$

are always satisfied [131]. The pair of dual filters $\gamma\phi$ and $\phi\gamma$ are called opening-closing and closing-opening filters, and they have almost the same filtering effects. Therefore, in practice, usually only one of them is employed.

In some applications, such as when the objects under processing are over a wide range of sizes, there is a need to alternatively use openings and closings with an SE of an increasing size. This sequential application of the basic operators is called an alternating sequential filter. Since the four types of sequential combinations of opening and closing are all morphological filters, four alternating sequential filters can be developed hereafter. Let γ_i and ϕ_i be a pair of dual operators with an SE of size i. Suppose the size of SE increases from i to j. Therefore, the four types of alternating sequential filters are given as:

$$f_{\text{aoc}} = (\gamma_j\phi_j)\cdots(\gamma_i\phi_i), \tag{2.30}$$

$$f_{\text{aco}} = (\phi_j\gamma_j)\cdots(\phi_i\gamma_i), \tag{2.31}$$

$$f_{\text{aoco}} = (\gamma_j\phi_j\gamma_j)\cdots(\gamma_i\phi_i\gamma_i), \tag{2.32}$$

$$f_{\text{acoc}} = (\phi_j\gamma_j\phi_j)\cdots(\phi_i\gamma_i\phi_i). \tag{2.33}$$

2.4 The Lifting Scheme and Morphological Wavelets

2.4.1 The Multi-resolution Decomposition Scheme

The multi-resolution decomposition scheme provides convenient and effective approaches for signal processing [97]. The core idea is to remove high frequencies in a signal, thus to obtain a reduced-scale version of the original signal. Therefore, by repeating this procedure, a collection of coarse signals at different levels are produced. Meanwhile, a collection of detail signals can be constructed by subtracting the coarse signal at level $i+1$ from the coarse signal at level i.

Let $J \subseteq \mathbb{N}$ be an index set indicating the levels in a multi-resolution decomposition scheme; J can be finite or infinite. Therefore, for a domain $V_j (j \in J)$, signals of level j belong to V_j. The analysis operator $\psi^{\uparrow}$ decomposes a signal in the direction of increasing, i.e. $\psi_j^{\uparrow} : V_j \to V_{j+1}$. On the other hand, the synthesis operator $\psi^{\downarrow}$ proceeds in the direction of decreasing, i.e. $\psi_j^{\downarrow} : V_{j+1} \to V_j$. In other words, the analysis operator $\psi^{\uparrow}$ maps a signal to a higher level and reduces information, while $\psi^{\downarrow}$ maps it to a lower level.

Composing analysis operators successively, a signal at any level i can be transferred to a higher level j. The composed analysis operator is denoted as $\psi_{i,j}^{\uparrow}$ and is defined to be:

$$\psi_{i,j}^{\uparrow} = \psi_{j-1}^{\uparrow}\psi_{j-2}^{\uparrow}\cdots\psi_i^{\uparrow}, \quad j > i. \tag{2.34}$$

It maps an element in V_i to an element in V_j. It should be noted that here the operations are carried from right to left. Likewise, the composed synthesis operator:

$$\psi_{j,i}^{\downarrow} = \psi_i^{\downarrow}\psi_{i+1}^{\downarrow}\cdots\psi_{j-1}^{\downarrow}, \quad j > i \tag{2.35}$$

takes the signal back from level j to level i. Finally, the composition operator that takes a signal from level i to level j and then back to level i is defined as:

$$\hat{\psi}_{i,j} = \psi_{j,i}^{\downarrow}\psi_{i,j}^{\uparrow}, \quad j > i, \tag{2.36}$$

where $\hat{\psi}_{i,j}$ is viewed as an approximation operator because analysis operator $\psi_j^{\uparrow}$ reduces signal information and, in general, the synthesis operator $\psi_j^{\downarrow}$ cannot compensate the information lost in the analysing procedure.

Analysis and synthesis operators play an important role in the construction of a decomposition scheme. If there is no information lost during the analysis and synthesis procedure, then this decomposition scheme would be perfect. The lifting scheme [136, 137] and morphological wavelets [55, 60] discussed in the next sections are designed to not modify the decomposition when the analysis and synthesis steps repeat.

2.4.2 The Lifting Scheme

The lifting scheme or simple lifting was originally developed as an alternative way to construct the wavelets used in (the first generation) WT, which leads to the so-called second generation WT [136, 137]. The second generation WT not only preserves the good features of the the first generation WT, namely time-frequency localisation and fast algorithms, but can also extend beyond simple geometries. As an alternate implementation of classical WTs, the lifting scheme provides an entirely spatial-domain interpretation of the transform, as opposed to the traditional frequency domain-based constructions. The feature of local spatial interpretation enables us to adapt the transform to the data, thereby introducing non-linearities in the process of multi-scale transforms. Compared with FTs using the same filter all the time and wavelets being translation and dilation of one given function, lifting adapts local data irregularities in the transform process.

The basic idea of the lifting scheme is very simple: the redundancy is removed by using the correlation in the data. To reach this goal, a signal x_k is first split into two sets – the even set $\{x_k | k \text{ is even}\}$ and the odd set $\{x_k | k \text{ is odd}\}$. Then, the odd set is predicted from the even set. Finally, the prediction error, which is the difference between the odd-indexed sample and its prediction, is used to update the even-indexed data. The three steps are noted as split, predict and update, respectively, as shown in Fig. 2.6.

1. *Split stage:* Let $x(n)$ represent a discrete signal. Firstly, $x(n)$ can be split into even and odd components, $x_{\mathrm{e}}(n)$ and $x_{\mathrm{o}}(n)$, respectively, where

$$\begin{aligned} x_{\mathrm{e}}(n) &= x(2n), \\ x_{\mathrm{o}}(n) &= x(2n+1). \end{aligned} \tag{2.37}$$

If the signal $x(n)$ corresponds to the sample of a smooth and slowly varying function, then the components of $x_e(n)$ and $x_o(n)$ are highly correlated. Therefore, it should be possible to accurately predict each odd polyphase coefficient from the nearby even polyphase coefficients.

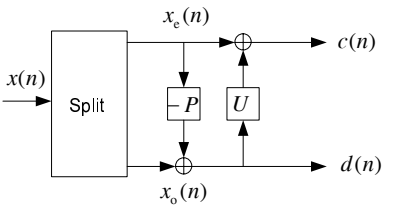

Fig. 2.6 The typical lifting steps (analysis): split, predict (P) and update (U). $c(n)$ and $d(n)$ are the approximation and detail signals, respectively

2. *Predict stage:* In the interpolating formulation of lifting, we can predict the odd polyphase coefficients $x_o(n)$ from the neighbouring even coefficients $x_e(n)$. Normally, the predictor for each $x_o(n)$ is a linear combination of neighbouring even coefficients:

$$P(x_e(n)) = \sum_l p_l x_e(n+l), \tag{2.38}$$

where the value of l lies on how many even coefficients are used for the prediction. If N ($N = 2D$) coefficients are used in symmetry, then:

$$-D+1 \le l \le D. \tag{2.39}$$

The prediction calculation is conducted within a data window of a fixed length. For each $x_o(n)$, its neighbouring even coefficients at both the left and right sides are involved in the calculation. As the window slides through the signal, the prediction for all odd coefficients is performed. If $n+l$ exceeds the range of the signal, the signal will be extended with zero samples, and this process is called zero padding.
A new representation of $x(n)$ may be obtained by replacing $x_o(n)$ with the prediction residual, $d(n)$:

$$d(n) = x_o(n) - P(x_e(n)). \tag{2.40}$$

The prediction residual will be small if the underlying signal is locally smooth. Furthermore, the same information of the original signal $x(n)$ is preserved in the residuals $d(n)$ since the odd polyphase coefficients $x_o(n)$ can be recovered by noting that

$$x_o(n) = d(n) + P(x_e(n)). \tag{2.41}$$

Actually, the prediction procedure is equivalent to applying a high pass filter to the original signal $x(n)$.

3. *Update stage:* The last lifting step transforms the even polyphase coefficients, $x_e(n)$, into a low pass filtered and sub-sampled version of $x(n)$ by updating $x_e(n)$ with a linear combination of the prediction residuals, $d(n)$, where $x_e(n)$ is replaced with

$$c(n) = x_e(n) + U(d(n)), \tag{2.42}$$

and normally $U(d)$ is a linear combination of the values of d:

$$U(d(n)) = \sum_l u_l d(n+l). \tag{2.43}$$

No information is lost in the update step. Assuming the same U is chosen for synthesis, given $d(n)$ and $c(n)$, we have

$$x_e(n) = c(n) - U(d(n)). \tag{2.44}$$

Following the description in WT, $d(n)$ is the detail signal obtained by the lifting scheme, while $c(n)$ is the approximation signal. Like WT, the aforementioned three stages are carried out on $c(n)$ recursively. The pseudo code of the lifting scheme is given in Table 2.5.

Table 2.5 The pseudo code of the lifting scheme

Denote the input signal $x(n)$ by $s_0(n)$. Set $k := 0$;
while (the end condition is not met)
  Split $s_{k,2l}(n) = s_k(2n)$;
    $s_{k,2l+1}(n) = s_k(2n+1)$;
  Predict Obtain the detail signal $d_{k+1,l}$:
    $d_{k+1,l}(n) = s_{k,2l+1}(n) - P(s_{k,2l}(n))$;
  Update Obtain the approximation signal $s_{k+1,l}$:
    $s_{k+1,l}(n) = s_{k,2l}(n) + U(d_{k+1,l}(n))$;
  $k := k+1$;
end

The inverse lifting stage is shown in Fig. 2.7. It corresponds to a critically sampled perfect reconstruction filter bank with c and d at half a rate.

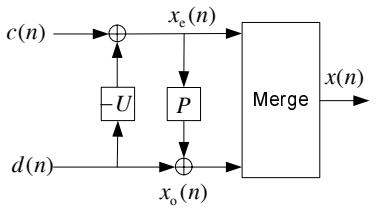

Fig. 2.7 The typical inverse lifting steps (synthesis): update (U), predict (P) and merge

As an example, the lifting scheme of the Harr wavelet and a family of Deslauriers–Dubuc wavelets are demonstrated here. The definitions of the first level are given as follows:

Harr:

$$\begin{aligned} d_{1,l} &= s_{0,2l+1} - s_{0,2l} \\ s_{1,l} &= s_{0,2l} + d_{1,l}/2 \end{aligned} . \tag{2.45}$$

Deslauriers–Dubuc:

$$\begin{aligned} (2,2): d_{1,l} &= s_{0,2l+1} - 1/2(s_{0,2l} + s_{0,2l+2}) \\ s_{1,l} &= s_{0,2l} + 1/4(d_{1,l-1} + d_{1,l}) \end{aligned} , \tag{2.46}$$

$$\begin{aligned} (4,2): d_{1,l} &= s_{0,2l+1} - [9/16(s_{0,2l} + s_{0,2l+2}) \\ &\quad -1/16(s_{0,2l-2} + s_{0,2l+4})] \\ s_{1,l} &= s_{0,2l} + 1/4(d_{1,l-1} + d_{1,l}) \end{aligned} , \tag{2.47}$$

$$\begin{aligned} (6,2): d_{1,l} &= s_{0,2l+1} - [75/128(s_{0,2l} + s_{0,2l+2}) \\ &\quad -25/256(s_{0,2l-2} + s_{0,2l+4}) \\ &\quad +3/256(s_{0,2l-4} + s_{0,2l+6})] \\ s_{1,l} &= s_{0,2l} + 1/4(d_{1-1,l} + d_{1,l}). \end{aligned} . \tag{2.48}$$

2.4.3 Morphological Wavelets

Most modern multi-resolution decomposition schemes are based on the pyramid and WT theories, using the convolution and time-frequency domain transformations. However, the linear filtering approaches to multi-resolution decomposition have not been theoretically justified. In particular, the operators used for generating various levels of signal components in a pyramid must crucially depend on an application. Therefore, in recent years, a number of researchers have proposed non-linear multi-resolution signal decomposition schemes based on morphological operators. The fundamental theories of the morphological pyramid [55] and the morphological wavelet [60] have built a framework for non-linear pyramids, filter banks and wavelets construction. They inherit the multi-dimension and multi-level analysis of wavelet and pyramid, while they do not require time-frequency domain analysis.

The morphological wavelet is a non-linear multi-resolution signal decomposition scheme [60]. It differs from ordinary multi-resolution decomposition schemes in that it engages two analysis operators and one synthesis operator. A formal definition of the morphological wavelet is presented as follows. Assume that there exist sets V_j and W_j. V_j is referred to as the signal space at level j and W_j the detail space at level j. The two analysis operators together decompose a signal in the direction of increasing j. The signal analysis operator, $\psi_j^{\uparrow}$, maps a signal from V_j to V_{j+1}, i.e. $\psi_j^{\uparrow} : V_j \to V_{j+1}$, while the detail analysis operator, $w_j^{\uparrow}$, maps it from V_j to W_{j+1}, i.e. $w_j^{\uparrow} : V_j \to W_{j+1}$. On the other hand, a synthesis operator proceeds in the direction of decreasing j, denoted as $\Psi_j^{\downarrow} : V_{j+1} \times W_{j+1} \to V_j$.

In order to yield a complete signal representation, the mappings $(\psi_j^{\uparrow}, \omega_j^{\uparrow}) : V_j \to V_{j+1} \times W_{j+1}$ and $\Psi_j^{\downarrow} : V_{j+1} \times W_{j+1} \to V_j$ should be inverses of each other, which means that the following condition:

$$\Psi_j^{\downarrow}(\psi_j^{\uparrow}(x), \omega_j^{\uparrow}(x)) = x,\ x \in V_j \tag{2.49}$$

should be fulfilled. This is called the perfect reconstruction condition, and

$$\begin{cases} \psi_j^{\uparrow}(\Psi_j^{\downarrow}(x,y)) = x,\ x \in V_{j+1}, y \in W_{j+1}, \\ \omega_j^{\uparrow}(\Psi_j^{\downarrow}(x,y)) = y,\ x \in V_{j+1}, y \in W_{j+1}, \end{cases} \tag{2.50}$$

where x is called the approximation signal and y is the detail signal. Therefore, decomposing an input signal $x_0 \in V_0$ with the following recursive analysis scheme:

$$x_0 \to \{x_1, y_1\} \to \{x_2, y_2, y_1\} \to \cdots \to \{x_j, y_j, y_{j-1}, \cdots, y_1\} \to \cdots \tag{2.51}$$

where

$$x_{j+1} = \psi_j^{\uparrow}(x_j) \in V_{j+1}, \tag{2.52}$$

$$y_{j+1} = w_j^{\uparrow}(x_j) \in W_{j+1}. \tag{2.53}$$

x_0 can be exactly reconstructed from x_j and $y_j,\ y_{j-1},\ \ldots,\ y_1$ by means of the following recursive synthesis scheme:

$$x_{j-1} = \Psi_{j-1}^{\downarrow}(x_j, y_j). \tag{2.54}$$

This signal representation scheme is referred to as the morphological wavelet decomposition scheme and is illustrated in Fig. 2.8.

2.4.3.1 The Morphological Haar Wavelet

To make the idea of morphological wavelet more concrete, a classic morphological wavelet called the morphological Haar wavelet (MHW) was introduced by [60]. MHW is different from the classical linear Haar wavelet in that the linear signal analysis operator of the classical Haar wavelet is replaced by a morphological operator, e.g. taking the minimum or maximum over two samples.

Let $V_j = V_{j+1} = W_{j+1} = \Re^{\mathbb{Z}}$ $(j \geq 0)$ be the lattice of doubly infinite real-valued sequences. In [60], the analysis and synthesis operators are defined as:

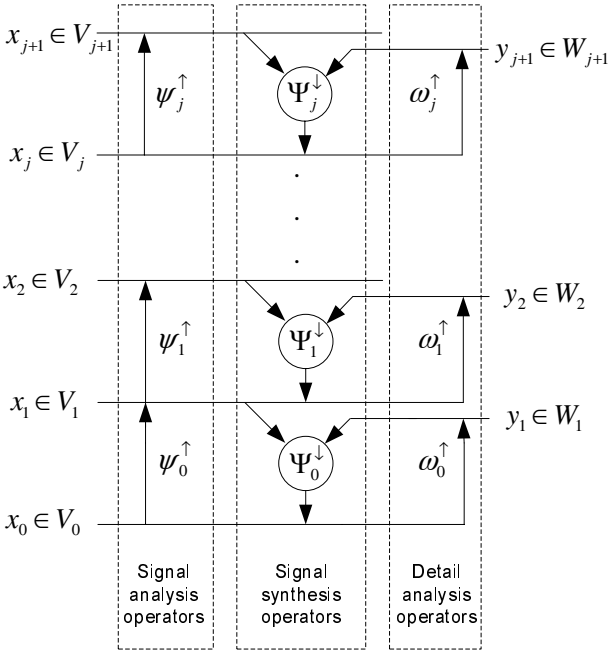

Fig. 2.8 Sample stages of the morphological wavelet decomposition scheme

$$\psi^{\uparrow}(x)(n) = x(2n) \wedge x(2n+1),\ x \in V_j, \tag{2.55}$$

$$\omega^{\uparrow}(x)(n) = x(2n) - x(2n+1),\ x \in V_j, \tag{2.56}$$

$$\begin{aligned} \psi^{\downarrow}(x)(2n) &= x(n),\ x \in V_{j+1}, \\ \psi^{\downarrow}(x)(2n+1) &= x(n),\ x \in V_{j+1}, \end{aligned} \tag{2.57}$$

$$\begin{aligned} \omega^{\downarrow}(y)(2n) &= y(n) \vee 0,\ y \in W_{j+1}, \\ \omega^{\downarrow}(y)(2n+1) &= -(y(n) \wedge 0),\ y \in W_{j+1}, \end{aligned} \tag{2.58}$$

$$\Psi^{\downarrow}(x,y)(n) = \psi^{\downarrow}(x)(n) + \omega^{\downarrow}(y)(n),\ x \in V_{j+1}, y \in W_{j+1}, \tag{2.59}$$

where n is the sample index, '$\wedge$' denotes the minimisation operation and '$\vee$' denotes the maximisation operation. Pseudo codes of the decomposition and reconstruction processes of MHW are listed in Tables 2.6 and 2.7, respectively. It is assumed here that the input signal is decomposed up to level K.

Table 2.6 The pseudo code of the decomposition process of MHW

Denote the input signal by $x_0(n)$. Set $k := 0$;
while $(k \leq K)$
  Get the analysis signal at level $k+1$: $x_{k+1}(n) = x_k(2n) \wedge x_k(2n+1)$;
  Get the synthesis signal at level $k+1$: $y_{k+1}(n) = x_k(2n) - x_k(2n+1)$;
  $k := k+1$;
end

Table 2.7 The pseudo code of the reconstruction process of MHW

Set $k := K$;
while $(k > 0)$
  Get the even samples at level $k-1$: $x_{k-1}(2n) = x_k(n) + (y_k(n) \vee 0)$;
  Get the odd samples at level $k-1$: $x_{k-1}(2n+1) = x_k(n) - (y_k(n) \wedge 0)$;
  $k := k-1$;
end

2.4.3.2 The Morphological Gradient Wavelet

The morphological gradient wavelet (MGW) is a morphological wavelet that aims to take into consideration the gradient of each sample of the signal. Derived from [48, 66], a morphological median operator termed by $\overset{\text{m}}{\oplus}$ is defined as:

$$(f \overset{\text{m}}{\oplus} g)(x) = \text{median}\{f(x-s) + g(s) | (x-s) \in \mathscr{D}_f, s \in \mathscr{D}_g\}, \tag{2.60}$$

where f is the signal, g is the SE, and $\mathscr{D}_f$ and $\mathscr{D}_g$ represent the definition domains of f and g, respectively. Apparently, instead of applying local minimum and maximum operations as dilation and erosion do, the morphological median operator returns the median value.

If the morphological median operator employs a flat SE whose length is 3 and whose origin is in the middle, (2.60) becomes:

$$(f \overset{\text{m}}{\oplus} g)(x) = \text{median}\{f(x-1), f(x), f(x+1)\}. \tag{2.61}$$

In MGW, the above equation is selected as the signal analysis operator, which is rewritten in (2.62). Consequently, the detail analysis operator of MGW is defined as depicted in (2.63).

$$\begin{aligned} \psi^{\uparrow}(x_j)(n) &= \text{median}\{x_j(2n-1), x_j(2n), x_j(2n+1)\} \\ &= x_{j+1}(n), \end{aligned} \tag{2.62}$$

$$\begin{aligned} \omega^{\uparrow}(x_j)(n) &= x_j(2n+1) - 2x_{j+1}(n) + x_j(2n-1) \\ &= y_{j+1}(n). \end{aligned} \tag{2.63}$$

In order to construct the synthesis operator, two intermediate variables are needed as follows:

$$t_{\mathrm{R},j+1}(n) = x_j(2n+1) - x_j(2n), \tag{2.64}$$
$$t_{\mathrm{L},j+1}(n) = x_j(2n) - x_j(2n-1), \tag{2.65}$$

where $t_{\mathrm{R},j+1}(n)$ and $t_{\mathrm{L},j+1}(n)$ denote the right and left gradient of $x_j(2n)$, respectively. The synthesis operator is shown in (2.66)–(2.68). Pseudo codes of the decomposition and reconstruction processes of MGW are listed in Tables 2.8 and 2.9, respectively. It is also assumed that the input signal is decomposed to level K.

$$\left.\begin{aligned} \Psi_j^{\downarrow}(2n) &= x_{j+1}(n) \\ \Psi_j^{\downarrow}(2n+1) &= x_{j+1}(n) + \tfrac{1}{2}(y_{j+1}(n) + \\ &\quad t_{\mathrm{R},j+1}(n) + t_{\mathrm{L},j+1}(n)) \end{aligned}\right\} \text{ if } t_{\mathrm{R},j+1} \cdot t_{\mathrm{L},j+1} \geq 0; \tag{2.66}$$

$$\left.\begin{aligned} \Psi_j^{\downarrow}(2n) &= x_{j+1}(n) + t_{\mathrm{L},j+1}(n) \\ \Psi_j^{\downarrow}(2n+1) &= x_{j+1}(n) + y_{j+1}(n) \end{aligned}\right\} \text{ if } \begin{array}{l} t_{\mathrm{R},j+1} \cdot t_{\mathrm{L},j+1} < 0 \text{ and} \\ |t_{\mathrm{R,j+1}}(n)| \geq |t_{\mathrm{L},j+1}(n)| \end{array}; \tag{2.67}$$

$$\left.\begin{aligned} \Psi_j^{\downarrow}(2n) &= x_{j+1}(n) + y_{j+1}(n) \\ &\quad + t_{\mathrm{L},j+1}(n) \\ \Psi_j^{\downarrow}(2n+1) &= x_{j+1}(n) \end{aligned}\right\} \text{ otherwise.} \tag{2.68}$$

Table 2.8 The pseudo code of the decomposition process of MGW

Denote the input signal by $x_0(n)$. Set $k := 0$;
while $(k \leq K)$
  Get the analysis signal at level $k+1$: $x_{k+1}(n) = \mathrm{median}\{x_k(2n-1), x_k(2n), x_k(2n+1)\}$;
  Get the synthesis signal at level $k+1$: $y_{k+1}(n) = x_k(2n+1) - 2x_{k+1}(n) + x_k(2n-1)$;
  Get the intermediate variables at level $k+1$: $t_{\mathrm{R},k+1}(n) = x_k(2n+1) - x_k(2n)$, $t_{\mathrm{L},k+1}(n) = x_k(2n) - x_k(2n-1)$;
  $k := k+1$;
end

Figure 2.9 shows the performance of MHW and MGW on a test signal [60]. To avoid misunderstanding, the approximation analysis operator and the detail analysis operator of MHW are denoted by $\psi_{\mathrm{H}}^{\uparrow}$ and $\omega_{\mathrm{H}}^{\uparrow}$, respectively, while those of MGW are denoted by $\psi_{\mathrm{G}}^{\uparrow}$ and $\omega_{\mathrm{G}}^{\uparrow}$, respectively. It can be seen that the detail signal obtained by $\omega_{\mathrm{H}}^{\uparrow}$ is zero at points where the input signal is constant, while that obtained by $\omega_{\mathrm{G}}^{\uparrow}$ is zero at points where the input signal is linear. Moreover, MGW not only detects every point where a change of gradient occurs, but also indicates the change quantitatively. These features make MGW suitable for the detection of sudden changes in

Table 2.9 The pseudo code of the reconstruction process of MGW

```
Set k := K;
while (k > 0)
  if t_{R,k} · t_{L,k} ≥ 0
    x_{k-1}(2n) = x_k(n)
    x_{k-1}(2n+1) = x_k(n) + 1/2 (y_k(n) + t_{R,k}(n) + t_{L,k}(n))
  else
    if |t_{R,k}(n)| ≥ |t_{L,k}(n)|
      x_{k-1}(2n) = x_k(n) + t_{L,k}(n)
      x_{k-1}(2n+1) = x_k(n) + y_k(n)
    else
      x_{k-1}(2n) = x_k(n) + y_k(n) + t_{L,k}(n)
      x_{k-1}(2n+1) = x_k(n)
    end
  end
end
```

gradient. As it can be seen from Fig. 2.9e, the impulses explicitly reveal the location where the gradient changes. On the contrary, for MHW, changes of gradient in the original signal correspond to changes in the amplitude in the detail signal, as shown in Fig. 2.9c. The gradient information is not distinctly presented in the detail signal, which means that in this situation MGW is more applicable than MHW.

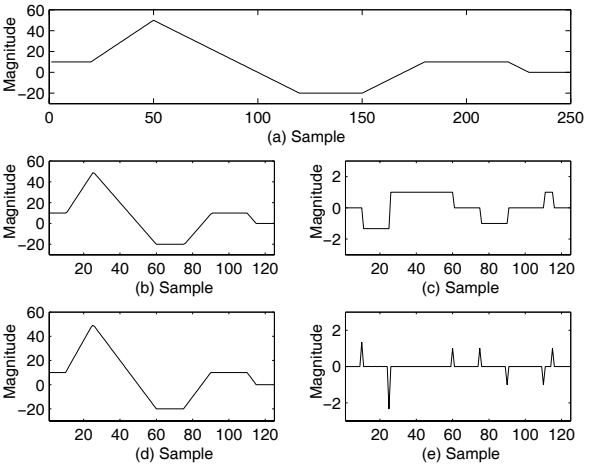

Fig. 2.9 The performance of MHW and MGW with analysis operators $\psi_{\mathrm{H}}^{\uparrow}, \omega_{\mathrm{H}}^{\uparrow}$ and $\psi_{\mathrm{G}}^{\uparrow}, \omega_{\mathrm{G}}^{\uparrow}$. **a** Original signal. **b** Approximation signal obtained by $\psi_{\mathrm{H}}^{\uparrow}$. **c** Detail signal obtained by $\omega_{\mathrm{H}}^{\uparrow}$. **d** Approximation signal obtained by $\psi_{\mathrm{G}}^{\uparrow}$. **e** Detail signal obtained by $\omega_{\mathrm{G}}^{\uparrow}$

2.4.4 The Multi-resolution Morphological Gradient Algorithm

The morphological gradient is defined as the arithmetic difference between the dilation and erosion of a signal by an SE. When using a flat SE, the morphological gradient is a powerful tool for edge detection. The multi-resolution morphological gradient (MMG) is an improved morphological gradient, which aims at depressing the steady state components and enhancing the transients ones. The multi-resolution morphological gradient algorithm (MMGA) introduced in this section is an algorithm designed to obtain the MMG of a signal, so that the ascending and descending edges of the transient waves can be extracted.

The morphological gradient is frequently used for edge detection in image and signal processing. Before giving its definition, two residual operators should be defined first. Denote the input signal and the SE by f and g, respectively. The dilation residual, G_{d}, is defined as the difference between the dilation of f by g and f, which is:

$$G_{\mathrm{d}}(f) = (f \oplus g) - f. \tag{2.69}$$

Similarly, we can define the erosion residual G_{e} to be the difference between f and the erosion of f by g, as follows:

$$G_{\mathrm{e}}(f) = f - (f \ominus g). \tag{2.70}$$

The morphological gradient is usually defined as:

$$G(f) = (f \oplus g) - (f \ominus g) = G_{\mathrm{d}}(f) + G_{\mathrm{e}}(f). \tag{2.71}$$

It should be noticed that there is a distinct meaning of morphological gradient, which is different from the gradient in physics. The geometric illustration and effect of the morphological gradient are depicted in Fig. 2.10, which demonstrates the process of the morphological gradient computation for a ramped-step signal, $f(x)$, by a flat SE, g, where the symbol $\triangle$ indicates the origin of the SE. Since dilation and erosion using a flat SE return the maximum and minimum of the neighbourhood, for every point, its morphological gradient reflects the difference between maximum and minimum obtained within the domain of the flat SE. Obviously, the morphological gradient is affected by the size and origin of the SE.

MMGA is designed based on the definition of the morphological gradient. In order to obtain the MMG, MMGA utilises a series of scalable flat SEs with different origins. The SEs are defined as:

$$g^{+} = \{0_1, 0_2, \ldots, 0_{l-1}, \underline{0_l}\}, \tag{2.72}$$

$$g^{-} = \{\underline{0_1}, 0_2, \ldots, 0_{l-1}, 0_l\}, \tag{2.73}$$

where g^{+} is the SE used for extracting the ascending edges and g^{-} is used for the descending edges of the signal; $l = 2^{1-a} l_g$, where a indicates the level of the MMG to be processed and l_g is the primary length of g at level 1; the underlined samples in g^{+} and g^{-} show their origins. Taking the definition in (2.71) as a reference, the

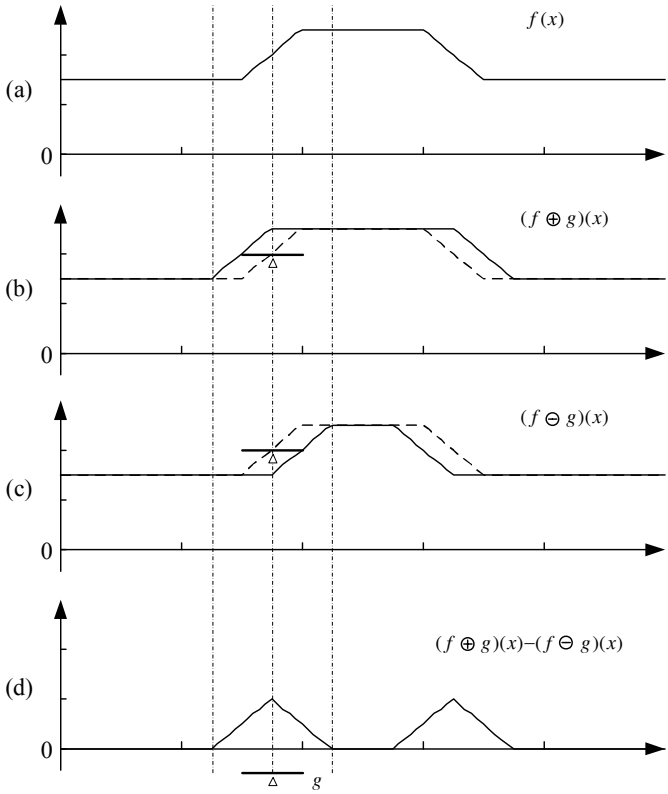

Fig. 2.10 The calculation and effect of the morphological gradient. **a** The input signal. **b** The dilation of f. **c** The erosion of f. **d** The morphological gradient

dyadic MMG at level a, ρ_g^a, is defined as:

$$\rho_{g^+}^a = (\rho^{a-1} \oplus g^+)(x) - (\rho^{a-1} \ominus g^+)(x), \tag{2.74}$$

$$\rho_{g^-}^a = (\rho^{a-1} \ominus g^-)(x) - (\rho^{a-1} \oplus g^-)(x), \tag{2.75}$$

$$\rho_g^a = \rho_{g^+}^a + \rho_{g^-}^a. \tag{2.76}$$

When $a = 1$, ρ^0 is the input signal. The pseudo code of MMGA is summarised in Table 2.10.

The explanations of (2.74) at level 1 is geometrically illustrated in Fig. 2.11. The solid lines in Figs. 2.11b and c are the results of dilation and erosion, respectively. For the purpose of comparison, the input signal is plotted with dashed lines. It is clear that under both transforms, the flat SE with the origin at its rightmost only affects the ascending edge of the input signal. This is because the origin of the flat SE should fall in the umbra of the input signal after either operation of dilation and erosion. Due to the geometrical symmetry of (2.74), there is no position shift-

Table 2.10 The pseudo code of MMGA

Denote the input signal by ρ^0. Determine the primary length l_g of the flat SE g. Set $a := 1$;
while (the end condition is not met)
  Construct the SEs:
    The length of the SE is $l_a = 2^{a-1} l_g$;
    $g^+(s) = \{0, 0, \cdots, 0\}$ and $1 - l_a \le s \le 0$;
    $g^-(s) = \{0, 0, \cdots, 0\}$ and $0 \le s \le l_a - 1$;
  Calculate the dilation and erosion of ρ^{a-1} by g^+ and g^-, respectively:
    $\delta_{a,+} = \rho^{a-1} \oplus g^+$
    $\delta_{a,-} = \rho^{a-1} \oplus g^-$
    $\varepsilon_{a,+} = \rho^{a-1} \ominus g^+$
    $\varepsilon_{a,-} = \rho^{a-1} \ominus g^-$
  Calculate the gradient:
    $\rho^a_{g^+} = \delta_{a,+} - \varepsilon_{a,+}$
    $\rho^a_{g^-} = \varepsilon_{a,-} - \delta_{a,-}$
    $\rho^a_g = \rho^a_{g^+} + \rho^a_{g^-}$
  $a := a + 1$;
end

ing introduced in the result illustrated in Fig. 2.11d. Likewise, the process of using MMGA to extract descending edges from the input signal is demonstrated in Fig. 2.12. In this case, the origin of the SE is at its leftmost as defined in (2.75) and MMGA is performed at level 1.

According to the ordering relation $(\rho^{a-1} \oplus g)(x) \ge (\rho^{a-1} \ominus g)(x)$, we have $\rho^a_{g^+} \ge 0$ in (2.74) and $\rho^a_{g^-} \le 0$ in (2.75), which correspond to the ascending and descending edges of the signal waveform. Thus, ρ^a_g in (2.76) is able to provide the information of not only the exact location of waveform changes but also their polarities (changing directions). An example to illustrate this is shown in Fig. 2.13.

2.5 Summary

This chapter has introduced in detail the fundamental concepts of MM and its operations and features. The basic morphological operators of dilation and erosion have been defined, both in binary and in grey scale. Some of their properties have also been presented, which may help readers understand the operators and further deliver the ideas of morphological filtering, opening and closing. The mathematical calculations involved in morphological operations include only addition, subtraction, maximum and minimum operations without any multiplication and division. Besides, MM uses a much smaller size of the sampling window in real-time signal processing, which is different from integral transform-based algorithms that require a period of the signal to obtain its main features. Since it is a time-domain signal processing method and does not perform any integral transforms, MM is applicable to non-periodic transient signals and not restricted to periodic signals. A more ex-

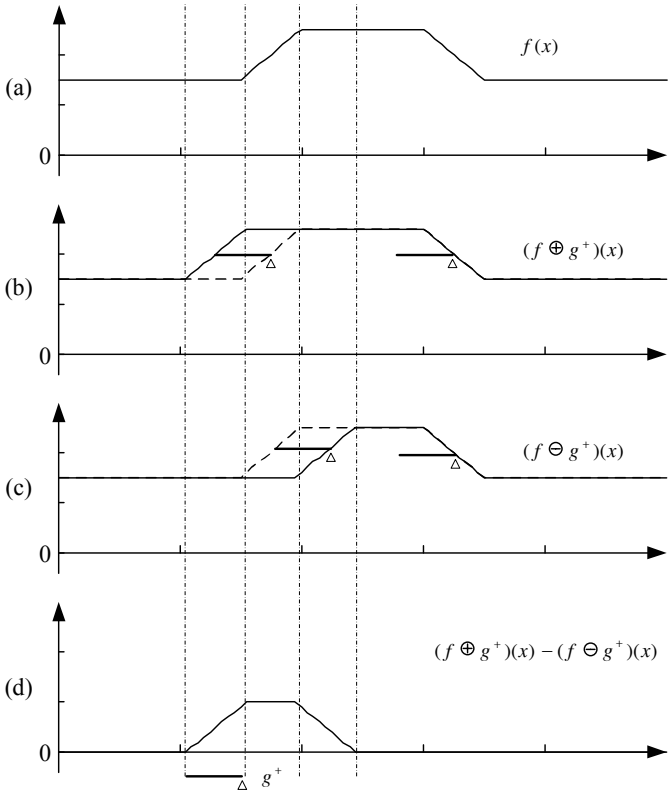

Fig. 2.11 The morphological gradient obtained by a flat SE with the origin at its rightmost. **a** The input signal. **b** The dilation of f. **c** The erosion of f. **d** The gradient at the first level

tensive discussion on MM can be found in the books by Matheron [99], Serra [125] and Soille [131], respectively.

MM has been mostly used in image processing; however, this book investigates MM for signal processing in particular. A large part of this chapter has been devoted to multi-resolution morphological operators, which are based on the framework of the multi-resolution decomposition scheme. This scheme provides us with an opportunity to view a signal at different levels. This chapter has introduced some classic operators, such as the lifting scheme, the morphological wavelet and MHW, as well as some operators that are derived from the classic methods, including MGW and MMGA. When acting upon signals of complex shapes, multi-resolution morphological operators are capable of decomposing a signal into meaningful parts and separating them from the background, while preserving the main shape characteristics.

In the following chapters, this book will show the application of MM to the development of novel algorithms for a variety of power system apparatus, including buses, transmission lines, and current transformers, etc. We will see that a group of

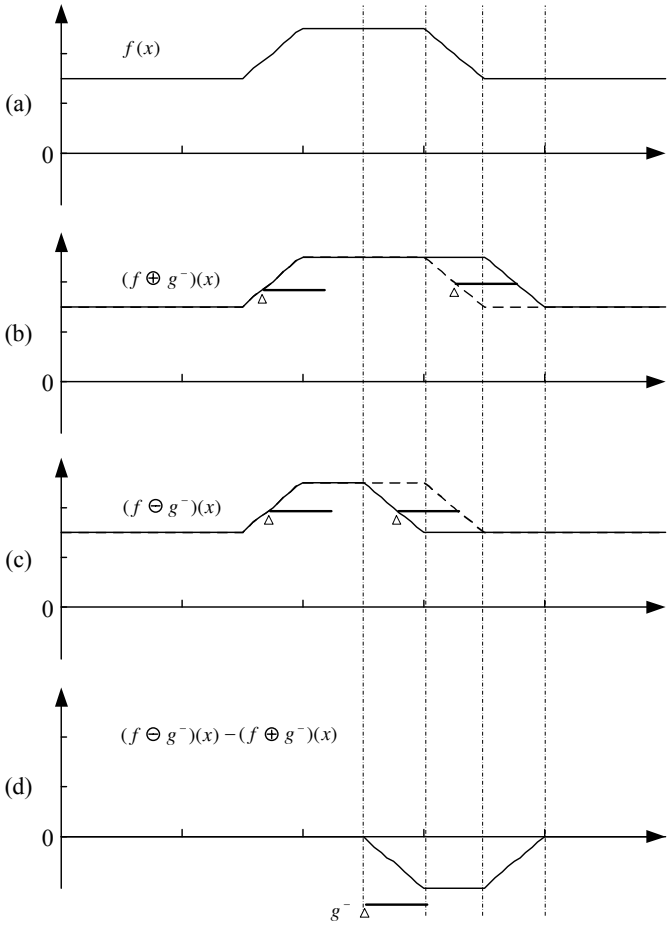

Fig. 2.12 The morphological gradient obtained by a flat SE with the origin at its leftmost. **a** The input signal. **b** The dilation of f. **c** The erosion of f. **d** The gradient at the first level

morphological operators have been developed specifically for protection algorithms, based on the operators and schemes introduced in this chapter.

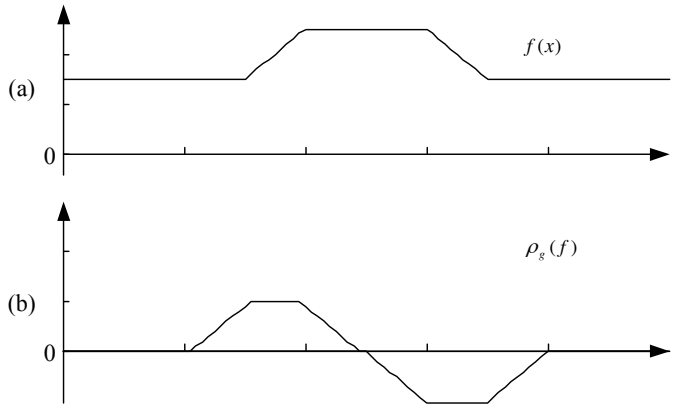

Fig. 2.13 A signal and its MMG at level 1. **a** The input signal. **b** Its MMG at level 1

Springer

http://www.springer.com/978-1-84882-498-0

Protective Relaying of Power Systems Using Mathematical Morphology

Wu, Q.H.; Lu, Z.; Ji, T.

2009, XXII, 208 p., Hardcover
ISBN: 978-1-84882-498-0